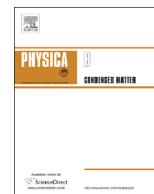




ELSEVIER

Contents lists available at ScienceDirect

Physica B

journal homepage: www.elsevier.com/locate/physb

Reaction kinetics of the double perovskite $\text{Sr}_2\text{FeMoO}_6$ by gas–solid reactions

J.L. Valenzuela^{a,b}, T.E. Soto^{b,c}, J. Lemus^a, O. Navarro^b, R. Morales^{a,*}

^a Instituto de Investigaciones Metalúrgicas, Universidad Michoacana de San Nicolás de Hidalgo, Ciudad Universitaria, Francisco J. Mújica S/N, Colonia Felicitas del Ro, C.P. 58030 Morelia, Mexico

^b Instituto de Investigaciones en Materiales, Universidad Nacional Autónoma de México, Apartado Postal 70-360, 04510 Mexico D.F., Mexico

^c Facultad de Ciencias Físico-Matemáticas, Universidad Michoacana de San Nicolás de Hidalgo, Ciudad Universitaria, Francisco J. Mújica S/N, Colonia Felicitas del Río, C.P. 58030 Morelia, Mexico

ARTICLE INFO

Article history:

Received 26 December 2013

Accepted 18 July 2014

Available online 30 July 2014

Keywords:

Double perovskite
Thermogravimetric
Strontium ferrate
Thermal decomposition

ABSTRACT

Double perovskite $\text{Sr}_2\text{FeMoO}_6$ is characterized by its colossal magnetoresistance, however, its production route is not well established. Therefore, the objective of this work is to study the reaction kinetics involved in the formation of $\text{Sr}_2\text{FeMoO}_6$. Firstly, precursor phases $\text{Sr}_2\text{Fe}_2\text{O}_5$ and SrMoO_4 were synthesized by gas–solid reactions from starting reagents such as SrCO_3 , Fe_2O_3 y MoO_3 . The thermogravimetric technique was employed to analyze the kinetics of formation of the double perovskite from the precursor phases given the optimized process variables. Microstructural characterization of the products obtained was performed by X-ray diffraction and Rietveld analysis. Results showed that the instability of $\text{SrFeO}_{2.5}$ during the reduction stage led to a formation of a disordered double perovskite $\text{Sr}_2\text{Fe}_{0.71}\text{Mo}_{1.29}\text{O}_6$.

© 2014 Elsevier B.V. All rights reserved.

1. Introduction

The double perovskite $\text{Sr}_2\text{FeMoO}_6$ (SFMO) has magnetotransport properties that have drawn attention in view of their application in magnetic recording devices [1]. This compound is half-metallic ferromagnetic oxide with colossal magnetoresistance (CMR) and Curie temperature of ~ 400 K [2,3]. The ordered lattice structure of SFMO consists of body centered cubic lattice with alternating FeO_6 and MoO_6 octahedra at the corners, strontium atom in its center [4]. In this configuration, the Fe has a +3 valence (spin quantum $S=5/2$) and Mo has +5 valence ($S=5/2$) with antiferromagnetic superexchange interaction between $S=5/2$ spins and $S=1/2$ spins which might produce the large ferromagnetic magnetization below T_C [2,5].

The most common method for the synthesis of SFMO is by solid state reaction, that is, calcination and reduction of initial reactants in controlled atmosphere [6–9]; TGA studies on the formation of SFMO are very limited; Jacobo et al. [10] performed a TGA experiment on precursor samples, prepared by wet chemical method towards the formation of SFMO, to only determine the water content in the sample. On the other hand, Hu et al. [11] showed that the ordering of the Fe and Mo cations in SFMO

structure improves with increasing sintering time. Kircheisen et al. [12] reported that the SFMO is stable between $10.2 \leq \log(p\text{O}_2) \leq -13.7$ at 1200°C below this range the SFMO is reduced into a lower oxide, and above that range, it decomposes into SrMoO_4 and SrFeO_{3-x} . This work studies the kinetics of the reactions for the formation of SFMO by thermogravimetric analysis (TGA) under well controlled experimental conditions.

2. Material and methods

Reagent powders of Fe_2O_3 (Alfa Aesar, 99.5%), SrCO_3 (Aldrich, 99.9%) and MoO_3 (Merck, 99.5%) were used to prepare separately the precursor phases $\text{SrFeO}_{2.5}$ ($\text{Sr}_2\text{Fe}_2\text{O}_5$) and SrMoO_4 (SMO). Reagent powders were first dried at 100°C for 10 h in a muffle furnace. Both the precursor powders were synthesized by weighing stoichiometric ratios of $\text{SrCO}_3/\text{Fe}_2\text{O}_3$ and $\text{SrCO}_3/\text{MoO}_3$. The powders were thoroughly mixed in an agate mortar for 30 min. Then, the powder mixtures were calcined in helium and then heated in a reducing atmosphere to form the double perovskite $\text{Sr}_2\text{FeMoO}_6$, the experimental details are explained below.

2.1. Thermogravimetry

To follow the gas solid reactions involved in the formation of $\text{Sr}_2\text{FeMoO}_6$, thermogravimetric analyses (TGA) were performed

* Corresponding author. Tel.: +52 443 3223554.

E-mail address: rmorales@umich.mx (R. Morales).

isothermally and nonisothermally using a Setaram, Setsys Evolution 16/18, which has an accuracy of 0.03 μg and is fully controlled through a personal computer. The calcination process was performed nonisothermally under a stream of helium gas (99.999%) with an oxygen concentration of $< 3 \times 10^{-6}$ atm. The reduction experiments were carried out in a mixture of 5% H_2 /He and 1.25% H_2 /He for nonisothermal and isothermal experiments, respectively. The purity of H_2 was 99.999%. 40 mg of powder sample was held into an alumina crucible (10 mm ID \times 1 mm H) which was hung from one end of the beam balance, using a 0.4 mm diameter Pt wire, and placed in the hot zone of the vertical furnace. The mass change during TGA experiments was recorded at 2 s intervals. The reactor furnace was made of dense alumina with an 18 mm inner diameter. The temperature of the furnace was controlled by a Pt–Pt/13% Rh (S-type) thermocouple placed just below the crucible. To perform nonisothermal experiments the analysis chamber was evacuated to less than 10 Pa, then the chamber was back filled with the desired working gas (He or H_2 /He). Once the atmospheric pressure was achieved, the reaction chamber was heated at a rate of 5 $^\circ\text{C}/\text{min}$ under a constant flow of the working gas of 100 ml/min. When the maximum temperature was reached, the furnace chamber was cooled down to room temperature at a maximum rate of 50 $^\circ\text{C}/\text{min}$ without changing the parameters of the working gas. For the isothermal reduction experiment, after the evacuation stage, the reaction chamber was heated at a rate of 40 $^\circ\text{C}/\text{min}$, under 40 ml/min of He gas, up to 1150 $^\circ\text{C}$. After the temperature in the chamber was stabilized, H_2 gas was led into the system for the reduction reaction to start. When no more significant weight loss was observed, the experiment was terminated manually allowing the furnace to reach room temperature in about 30 min. The reducing atmosphere was kept during the cooling stage to avoid oxidation of the sample.

2.2. X-ray diffraction and Rietveld refinement

Calcined and reduced samples were structurally studied by X-ray diffraction (XRD) using a Siemens D-5000 diffractometer at 30 mA, 50 kV and 0.2 $^\circ$ /12 s step size with $\text{Cu K}\alpha$ radiation. Rietveld method was employed for the determination of the crystalline structure using a computer software GSAS (Toby, 2001). The structures used for refinement were $\text{Sr}_2\text{Fe}_{0.8}\text{Mo}_{1.2}\text{O}_6$ and $\text{SrFeO}_{2.7341}$ that correspond to the Powder Diffraction Files (PDF) 98-006-9936 and 98-010-5739, respectively.

3. Results

The weight loss obtained from the calcination experiments of mixtures of $\text{SrCO}_3/\text{MoO}_3$ and $\text{SrCO}_3/\text{Fe}_2\text{O}_3$ powders indicated the complete formation of SMO and $\text{SrFeO}_{2.5}$ precursor phases, respectively. These findings were confirmed by XRD analyses as seen in Fig. 1.

The obtained Bragg peaks revealed that the precursor phases were highly crystalline and matched the reference patterns of $\text{SrFeO}_{2.5}$ ($\text{Sr}_2\text{Fe}_2\text{O}_5$) (PDF: 98-000-3411) and SrMoO_4 (PDF: 98-000-7961); no other phases were detected in each precursor phase.

The nonisothermal reduction of the mixed precursors is shown in Fig. 2, the total weight loss from room temperature up to 1250 $^\circ\text{C}$ was 7.5%. To understand the process of weight loss in the reduction of the double perovskite, each precursor was reduced separately as shown in Fig. 3. As it can be seen the weight loss for SMO suggests that the reduction reaction starts at about 850 $^\circ\text{C}$ and ends about 1150 $^\circ\text{C}$, in contrast, the weight loss of $\text{SrFeO}_{2.5}$ starts from room temperature and keeps losing weight at the end of the heating cycle.

Fig. 4 shows the percentage weight loss curves of the $\text{SrFeO}_{2.5}$ for different atmospheres, it can be seen that the oxide phase loses weight from very low temperatures independent of the atmosphere.

Based on the above preliminary experiments, the optimum process parameters were chosen to perform an isothermal reduction experiment as shown in Fig. 5. It is clearly seen that after 120 min, the reduction reaction seemed to keep losing weight at a very low rate.

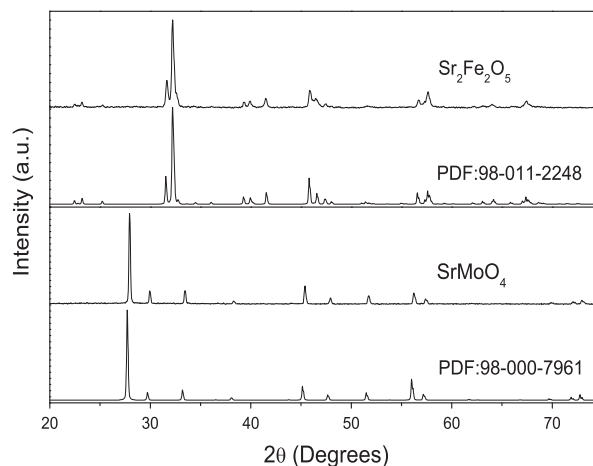


Fig. 1. XRD results of the precursor powders $\text{SrFeO}_{2.5}$ and SrMoO_4 obtained by calcination of the reagents $\text{SrCO}_3/\text{Fe}_2\text{O}_3$ and $\text{SrCO}_3/\text{MoO}_3$, respectively. Also shown are the corresponding reference standards.

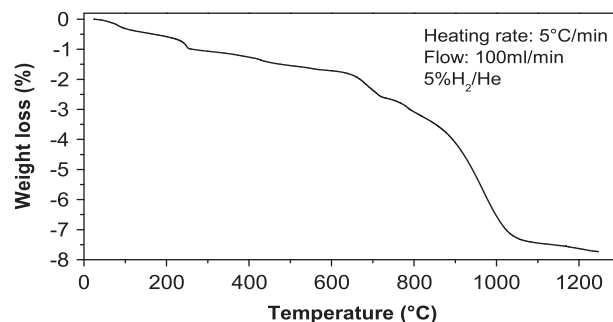


Fig. 2. Nonisothermal reduction curve of mixed precursors, SMO and $\text{SrFeO}_{2.5}$, by TGA.

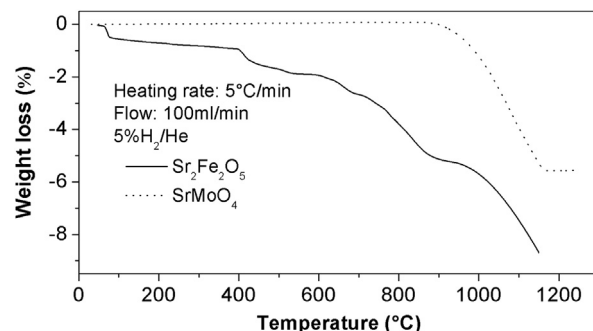


Fig. 3. Kinetic behavior of precursor phases, SrMoO_4 and $\text{Sr}_2\text{Fe}_2\text{O}_5$, under non-isothermal reducing conditions.

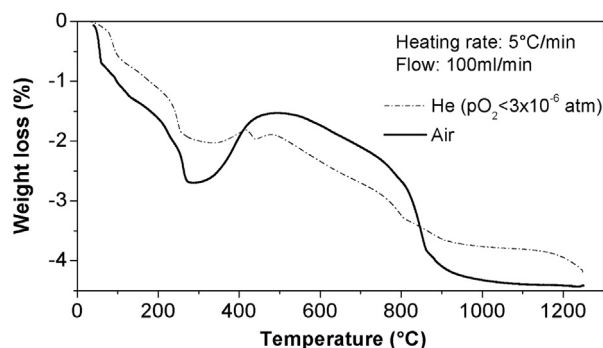


Fig. 4. Nonisothermal treatment of $\text{Sr}_2\text{Fe}_2\text{O}_5$ under different atmospheres.

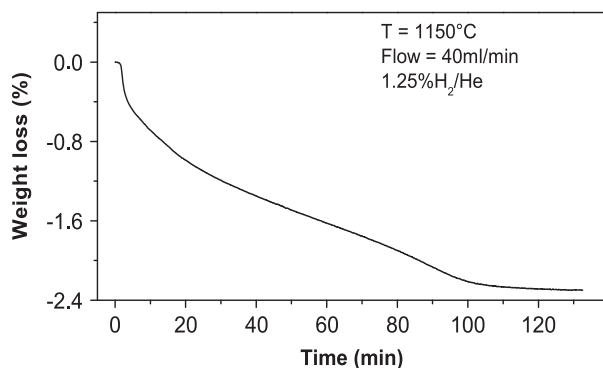


Fig. 5. Isothermal reduction curve of mixed precursor phases towards the formation of $\text{Sr}_2\text{FeMoO}_6$.

4. Discussion

A theoretical general equation for the reduction of a two phase mixture, $\text{SrFeO}_{2.5}$ and SrMoO_4 , with hydrogen is given by Reaction 1. For Reaction 1 to be completed successfully, a theoretical weight loss of 1.98% was calculated.

The isothermal experiments presented in Fig. 5 show that the observed weight loss is about 2.35%. This value is not close to the theoretical one. On the other hand, the weight loss observed in the nonisothermal experiment, i.e. 7.1%, is too large suggesting that the reduction process does not follow Reaction 1. Therefore, nonisothermal experiments were discarded:



It should be noted that most of the published works on the synthesis of $\text{Sr}_2\text{FeMoO}_6$, by solid state reaction, do not discuss the theoretical weight loss against the experimental one. Nevertheless, the difference in the weight loss, between the isothermal experiment and the theoretical given by Reaction 1, calls for an explanation. As it can be seen in Fig. 3, $\text{SrFeO}_{2.5}$ starts to lose weight from very low temperatures; this event cannot be attributed to moisture in the sample but rather to the loss of oxygen atoms. It is well documented that SrFeO_{3-x} has a high mobility of oxygen at lower temperatures [13,14]. Similarly, the oxygen nonstoichiometry of SrFeO_{3-x} is greatly influenced by temperature and p_{O_2} in the system [15]. The results in Fig. 4 confirm that the $\text{SrFeO}_{2.5}$ is quite unstable regardless of the p_{O_2} in the system. Therefore the behavior of $\text{SrFeO}_{2.5}$ in reducing conditions (Fig. 3) is to be expected. Because $\text{SrFeO}_{2.5}$ is already partially reduced before higher temperatures are achieved, the stoichiometry of reactants is misadjusted at the time enough energy is available to allow the occurrence of Reaction 1.

Theoretically, the formation of SFMO should start as soon as SrMoO_4 is reduced by H_2 to $\text{SrMoO}_{3.5}$ so that the Mo valence changes from 6^+ to 5^+ , then the latter phase reacts with $\text{SrFeO}_{2.5}$ in the solid state to form $\text{Sr}_2\text{FeMoO}_6$. To diminish the earlier reduction of $\text{SrFeO}_{2.5}$, isothermal experiments had to be executed with a high heating rate in He atmosphere up to the isothermal reduction temperature. Then, a low concentration of H_2 was introduced in the system at a low flow rate to decrease the kinetics of reduction of $\text{SrFeO}_{2.5}$ and SrMoO_4 .

The XRD analysis carried out on the products obtained from the isothermal experiment (Fig. 5) is shown in Fig. 6. It could be realized that there was a good fit between the observed and the reference patterns of $\text{Sr}_2\text{FeMoO}_6$ (PDF:98-010-2385). However, Rietveld analysis failed to refine the diffraction data to a single phase; therefore, two phases had to be considered as shown in the enlarged areas in Fig. 6.

Table 1 shows the computed values of lattice parameters, from Rietveld refinement, of the two phases found which are referred in terms of x . Table 1 also includes lattice parameters of target compounds for comparison purposes. It is clearly seen that as the amount of atomic Fe is decreased in the double perovskite, the lattice parameters a and b tend to decrease. This behavior should be expected as Fe sites are occupied by Mo atoms which have a smaller atomic radius (0.64 Å vs 0.62 Å). The quantities in weight percent of phase 1 ($\text{Sr}_2\text{Fe}_{0.8-x}\text{Mo}_{1.2+x}\text{O}_6$) and phase 2 ($\text{SrFeO}_{2.7035}$) obtained by Rietveld refinement were 79.1% and 20.9%, respectively.

Reaction 1 was then rewritten into Reaction 2 to account for the experimental weight loss observed (2.35%), the amount of each phase described by Rietveld refinement, and experimental error. Therefore, a value of x close to 0.09 in phase $\text{Sr}_2\text{Fe}_{0.8-x}\text{Mo}_{1.2+x}\text{O}_6$ (Table 1) would

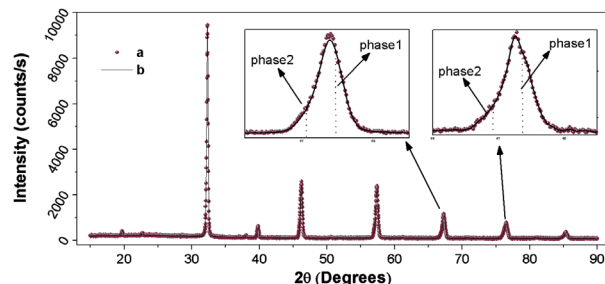


Fig. 6. (a) X-ray diffraction pattern and (b) Rietveld refinement, with two structural phases, $\text{Sr}_2\text{Fe}_{0.8}\text{Mo}_{1.2}\text{O}_6$ and $\text{SrFeO}_{2.7341}$, of products obtained in Fig. 5.

Table 1

Lattice parameters and weight percentage of products obtained, from isothermal reduction of mixed precursor phases (Fig. 5), by Rietveld refinements.

Compound	Lattice parameter			Wt(%)
	a (Å)	b (Å)	c (Å)	
Phase 1				
$\text{Sr}_2\text{Fe}_{0.8-x}\text{Mo}_{1.2+x}\text{O}_6$	5.573	5.573	7.903	79.1
$\text{Sr}_2\text{Fe}_{0.8}\text{Mo}_{1.2}\text{O}_6^a$	5.575	5.575	7.903	
$\text{Sr}_2\text{FeMoO}_6^b$	5.583	5.583	7.882	
Phase 2				
$\text{SrFeO}_{(2.7035)}$	7.926	7.926	7.926	20.9
$\text{SrFeO}_{2.7341}^c$	7.852	7.852	7.852	

Lattice parameters taken from Powder Diffraction Files for comparison purposes.

^a PDF:98-006-9936.

^b PDF:98-010-2385.

^c PDF:98-010-5739.

meet the above criteria. The value of x would depend upon the early reduction behavior of the precursor phase $\text{SrFeO}_{2.5}$ in the synthesis of $\text{Sr}_2\text{FeMoO}_6$:



5. Conclusions

This work illustrates that the oxygen-vacancy precursor SrFeO_{3-x} plays an important role in the solid state synthesis of $\text{Sr}_2\text{FeMoO}_6$. The oxygen nonstoichiometry of SrFeO_{3-x} is very sensitive to temperature and oxygen partial pressure in the system. Thus, care must be exercised in selecting the process parameters that affect the route of synthesis and in determining correct crystal structures of the end products. In the prevailing reducing conditions, which are the most generally adopted, during the synthesis of $\text{Sr}_2\text{FeMoO}_6$ the oxygen stoichiometry in the $\text{SrFeO}_{2.5}$ phase decreases as temperature increases leading to a disordered double perovskite $\text{Sr}_2\text{Fe}_{0.71}\text{Mo}_{1.29}\text{O}_6$ and $\text{SrFeO}_{2.7035}$.

Acknowledgments

This work was partially supported by CONACyT Grant 131589 and PAPIIT-IN100313 from UNAM. T.E. Soto and J.L. Valenzuela thank CONACyT.

References

- [1] T.-T. Fang, J.-C. Lin, *Mater. Sci.* 40 (2005) 683–686.
- [2] K.-I. Kobayashi, T. Kimura, H. Sawada, K. Terakura, Y. Tokura, *Nature* 395 (1998) 1609–1610.
- [3] J. Suárez, F. Estrada, O. Navarro, M. Avignon, *Eur. Phys. J. B* 84 (2011) 53–58.
- [4] D. Topwal, D.D. Sarma, H. Kato, Y. Tokura, M. Avignon, *Phys. Rev. B* 73 (2006) 094419.
- [5] Y. Lin, X. Chen, X. Liu, *Solid State Commun.* 149 (2009) 784–787.
- [6] R. Chang, W. College, M. Medeles, R. Herranz, *Química*, McGraw-Hill, 2002.
- [7] T.-T. Fang, M.S. Wu, T.F. Ko, *Mater. Sci. Lett.* 20 (2001) 1609–1610.
- [8] J.M. Greneche, M. Venkatesan, R. Suryanarayanan, J.M.D. Coey, *Phys. Rev. B* 63 (2001) 174403.
- [9] D. Sarma, *Solid State Commun.* 114 (2000) 465–468.
- [10] S.E. Jacobo, *Mater. Sci.* 40 (2005) 417–421.
- [11] Y.C. Hu, J.J. Ge, Q. Ji, B. Lv, X.S. Wu, G.F. Cheng, *Powder Diffr.* 25 (2010) S17–S21.
- [12] R. Kirchseisen, J. Topfer, *J. Solid State Chem.* 185 (2012) 76–81.
- [13] J. Köhler, *Angew. Chem. Int. Ed.* 47 (2008) 4470–4472.
- [14] J. Yoo, A.J. Jacobson, in: *Proceedings of the Electrochemical Society*, 2003, PV2002–26 354.
- [15] Y. Takeda, K. Kanno, T. Takada, O. Yamamoto, M. Takano, N. Nakayama, Y. Bando, *J. Solid State Chem.* 63 (1986) 237–249.